

# RSC Advances



This is an *Accepted Manuscript*, which has been through the Royal Society of Chemistry peer review process and has been accepted for publication.

*Accepted Manuscripts* are published online shortly after acceptance, before technical editing, formatting and proof reading. Using this free service, authors can make their results available to the community, in citable form, before we publish the edited article. This *Accepted Manuscript* will be replaced by the edited, formatted and paginated article as soon as this is available.

You can find more information about *Accepted Manuscripts* in the [Information for Authors](#).

Please note that technical editing may introduce minor changes to the text and/or graphics, which may alter content. The journal's standard [Terms & Conditions](#) and the [Ethical guidelines](#) still apply. In no event shall the Royal Society of Chemistry be held responsible for any errors or omissions in this *Accepted Manuscript* or any consequences arising from the use of any information it contains.

**A nano-sized solid acid synthesized from rice hull ash for biodiesel production**

Danlin Zeng\*, Shenglan Liu, Wanjun Gong, Hongxiang Chen and Guanghui Wang

---

*College of Chemical Engineering and Technology, Hubei Key Laboratory of Coal Conversion and New Carbon Material, Wuhan University of Science and Technology, Wuhan 430081, China.*

*E-mail: zdanly@163.com; Fax: +86 27 6886 2181; Tel: +86 27 6886 2181*

**Abstract:** A nano-sized solid acid was synthesized from rice hull ash by acid activation. The solid acid was characterized by XRD, FT-IR, TEM and Solid-state NMR spectroscopy. The characterization results show that the solid acid is the amorphous silica with -OH and -SO<sub>3</sub>H functional acid groups. The TEM images display the particle size range of the solid acid catalyst is 50-100 nm. In addition, the catalytic results indicate that the solid acid exhibits excellent activity and recyclability for the transesterification reaction of soybean oil with methanol, suggesting promising industrial applications in biodiesel production.

Keywords: solid acid; rice hull ash; catalyst; biodiesel

## 1. Introduction

Liquid acids ( $\text{H}_2\text{SO}_4$ , HF or  $\text{H}_3\text{PO}_4$ ) generate serious problems such as dangerous transportation, difficult separation, waste acid pollution and strong corrosivity in industrial application.<sup>1-4</sup> Though the base-catalyzed transesterification is relatively faster than the acid catalyzed transesterification, the base catalyst is sensitive to the oil of high free fatty acid (FFA) content, which greatly limits the raw materials of biodiesel.<sup>5</sup> Consequently, the research on solid acid catalyst has been paid considerable attention in acid catalysis because of their environmental, economical and operational advantages.<sup>6</sup> In the past decades several solid acids have been synthesized and used in acid catalysis reactions. Inorganic-oxide solids such as zeolites,<sup>7</sup> niobic acid,<sup>8,9</sup> strong acidic ion exchange resins,<sup>10,11</sup> sulfonated zirconia and carbon-based materials are the typical solid acids which have been extensively investigated.<sup>12-15</sup> These solid acids have attracted a great deal of attention due to their easy operation, good catalytic efficiency and high selectivity in the catalysis reaction. One useful example of reusable heterogeneous solid acid is silica sulfuric acid, which exhibits excellent efficiency in lots of acid catalysis reactions.<sup>16,17</sup> This solid acid can be easily synthesized from the treatment of silica gel at moderate temperature.<sup>18</sup>

Rice hull, an agro-based waste, is normally disposed of by burning in the field which results in environmental pollution in China. Rice hull ash (RHA) prepared by calcination rice hull under air was been found to be an economically viable raw material for the production of silicates and silica.<sup>19-22</sup> It is necessary to explore the possibility of using this low cost silica to prepare solid acid for heterogeneous

catalysis.

In this work, rice hull ash was used as the starting material to prepare silica-based solid acid catalyst for biodiesel production from soybean oil and methanol. A nano-sized solid acid was synthesized from rice hull ash by NaOH leaching and concentrated H<sub>2</sub>SO<sub>4</sub> activation. The solid acid catalyst was also characterized by X-ray diffraction (XRD), Fourier-transform infrared spectra (FT-IR), transmission electron microscope (TEM) and solid state nuclear magnetic resonance (NMR) spectroscopy. The characterization results will be helpful to obtain the fundamental information of the roles of surface functional groups in the solid acid, which is crucial in the design of a novel silica-based solid acid for industrial application.

## **2. Experimental**

### **2.1. Catalyst preparation**

#### **2.1.1 Solid acid from rice hull ash**

Rice hull was obtained from a grain depot in Wuhan, China. Rice hull was heated at 10 °C/min in three-stages, first to 150 °C and held for 1 h, then to 325 °C and stayed for another 1 h, finally to 575 °C and held for 10 h in air to remove the organics and resultant carbon. The product, in the form of white ash, was collected, sealed in a plastic bottle and stored at room temperature for the following experiment and analysis. The chemical composition of the rice hull ash is listed in Table 1, which was determined by atomic emission measurements using inductively coupled plasma (ICP) emission spectroscopy (Spectro Analytical Instruments).

NaOH solution (1 M) was added to the rice hull ash samples with a solid to liquid ratio of 1:5 and boiled for 1 h with constant stirring to dissolve the silica and produce a sodium silicate solution. The solutions were filtered, and then washed with 100 ml of boiling water. The filtrates and washings were allowed to cool to room temperature and were titrated with 0.1 M HNO<sub>3</sub> with constant stirring to pH 7. Silica gels were started to precipitate when the pH decreased slowly. The produced silica gels were aged for 12 h, centrifuged, and then the gels were transferred into a beaker and dried at 150 °C for 12 h to produce silica. The silica sample which was calcined at 1000 °C for 12 h was also prepared to characterize its phase transformation.

To prepare the solid acid, the silica gels (SiO<sub>2</sub>, 99.6wt%; calcined at 150 °C ) were activated with concentrated H<sub>2</sub>SO<sub>4</sub> (98wt%), at 200 °C under a N<sub>2</sub> flow (10mL/min) for 10 h at a ratio of solid to liquid of 1 g: 100 mL. At last, the mixture was diluted with deionized water, filtered, washed thoroughly, and dried at 150 °C for 12 h to obtain the solid acid catalyst (SiO<sub>2</sub>, 99.0wt%). All the samples were stored in airtight plastic bottles.

### 2.1.2 SO<sub>4</sub><sup>2-</sup>/ZrO<sub>2</sub> catalyst

As a typical solid acid, SO<sub>4</sub><sup>2-</sup>/ZrO<sub>2</sub> catalyst was used to perform a comparative study. The SO<sub>4</sub><sup>2-</sup>/ZrO<sub>2</sub> catalyst in this work was prepared using the classic two-step method.

<sup>23</sup> Zirconium hydroxide was prepared by hydrolysis of zirconyl chloride (ZrOCl<sub>2</sub>·H<sub>2</sub>O, 99%, Merk) with aqueous ammonia, and then SO<sub>4</sub><sup>2-</sup>/ZrO<sub>2</sub> catalyst was prepared by impregnation method. Zirconium hydroxide fractions were soaked with 1 M sulfuric

acid solution with stirring for 1 h at room temperature. The H<sub>2</sub>SO<sub>4</sub>-impregnated zirconium hydroxide sample was dried at 400 °C in air for 24 h to obtain SO<sub>4</sub><sup>2-</sup>/ZrO<sub>2</sub> catalyst.

## 2.2. Sample characterization

The concentration of acid sites on the catalysts was determined by titration method in aqueous solution. One gram of the sample was placed in 50 ml of 0.05 M NaOH solution. The vials were sealed and shaken for 24 h and then 5 ml of the filtrate was pipetted and the excess of base was titrated with HCl. The numbers of acidic sites were calculated from the amount of NaOH that reacted with the catalyst.

Surface area and porosity properties of samples were evaluated by N<sub>2</sub> adsorption/desorption isotherms carried out at 77 K on a Micromeritics ASAP 2020 sorption analyzer. Prior to the adsorption–desorption measurements, all the samples were degassed at 150 °C in N<sub>2</sub> flow (50mL/min) for 12 h.

The FT-IR spectra were recorded on Impact 410, Nicolet spectrometer with a resolution of 2 cm<sup>-1</sup>. 12 mg of each sample was pressed into a self-supported wafer 16 mm in diameter. The wafers were heated at 200 °C in an IR cell under vacuum (<10<sup>-3</sup> Pa) for 4 h before the IR spectra of the samples were measured.

X-ray diffraction (XRD) was performed with a Philips X'PERT-Pro-MPD diffractometer, operating with Cu K $\alpha$  radiation (40 kV, 30 mA) and Ni filter.

The TEM (Transmission electron microscope) images were taken over a JEOL JEM-2000EX instrument operated at 80 kV.

All the NMR experiments were carried out at 9.4 T on a Varian Infinityplus-400

spectrometer with resonance frequencies of 400.12, 100.4, 161.9 MHz for  $^1\text{H}$ ,  $^{13}\text{C}$ ,  $^{31}\text{P}$ , respectively. The  $90^\circ$  pulse widths for  $^1\text{H}$ ,  $^{13}\text{C}$ ,  $^{31}\text{P}$  were measured to be 3.7, 4.4, 3.6  $\mu\text{s}$ , respectively. The chemical shifts were referenced to tetramethylsilane (TMS) for  $^1\text{H}$ , to hexamethylbenzene (HMB) for  $^{13}\text{C}$ , to 85%  $\text{H}_3\text{PO}_4$  solution for  $^{31}\text{P}$ , respectively. Repetition times of 6 s for  $^1\text{H}$ , 60 s for  $^{31}\text{P}$  single-pulse experiments were used. The magic angle spinning rate was 5 kHz.

For the adsorption of probe molecules trimethylphosphine (TMP), samples were kept at 673 K under the vacuum less than  $1 \times 10^{-3}$  Pa for at least 8 h. The adsorption of TMP was performed at room temperature with a loading of about 0.1 mmol per gram catalyst. The adsorption procedure of trimethylphosphine oxide (TMPO) was different from that of TMP. About 0.5 g of dehydrated sample was mixed with 3 ml  $\text{CH}_2\text{Cl}_2$  solution containing 0.1 M TMPO in a glove box before the mixture was stirred for 3 h by an ultrasonic shaker, equilibrated for 5 h, and then evacuated under vacuum to remove  $\text{CH}_2\text{Cl}_2$  and excess TMPO before NMR measurements.

### 2.3. The procedure for the biodiesel synthesis

**2.3.1 Soybean oil.** Food-grade soybean oil supplied by commercial supermarket was used to carry out the transesterification reaction. According to GC (HP6890) analysis, the fatty acid compositions of the used soybean oil were as follows: palmitic acid, 12.5 wt%; stearic acid, 5.9 wt%; oleic acid, 26.6 wt%; linoleic acid, 49.9 wt%; and linolenic acid, 5.4 wt%. The water content of the oil was reduced to lower than 10 ppm. The average molecular weight of the oil is 850.

**2.3.2 Transesterification.** The transesterification of soybean oil with methanol was



carried out by using solid acid catalyst prepared from the rice hull ash. A 250 mL glass flask with a water-cooled condenser was charged with 8.74 g (10.0 mmol, calculated from the average molecular weight of soybean oil) of soybean oil, 3.84 g of anhydrous methanol (120 mmol) and 0.015 g of catalyst. The mixture was vigorously stirred with a magnetic stirrer. All of the transesterification reactions were performed under reflux, vapor from the reaction mixture being condensed by cold water (about 10 °C). After the transesterification reaction finished, the mixture was filtered and the residual methanol was separated from the liquid phase via rotary evaporation.

**2.3.3 Analysis.** Analysis of the reaction mixtures was carried out in a HP 6890 series gas chromatograph equipped with a flame ionization detector (FID). The solgel premium capillary column (30 m × 0.25 mm × 0.25 μm) was used in the analysis. At first, the oven was kept at 180 °C for 5 min, and then increased to 210 °C at a rate of 3 °C /min. The injection volume of all the samples was 0.2 μL. The inlet temperature was 250 °C, and the detector temperature was 270 °C. TOF (Turn over frequency) was calculated on the data of the mol of converted reactant, the mol of acid sites and reaction equilibrium time.

**2.3.4 Recycling.** Recycling experiments were performed to determine the catalytic stability of the solid acid catalysts. At the end of each cycle, the same catalyst was directly used for next time without any pretreatment. The spent solid acid was obtained after 10 recycle times using. Then the spent solid acid was washed with acetone, dried at 120 °C under the vacuum for 5 h to obtain the regenerated solid acid. Pore structure and total acid density of rice hull ash and solid acid from rice hull ash

(fresh, spent and regenerated) are listed in Table 2.

### 3. Results and discussion

#### 3.1. Catalyst characterization

##### 3.1.1 XRD analysis

Fig. 1 illustrates the XRD patterns of the rice hull ash, silica from rice hull ash and the solid acid. The broad diffraction peaks arising at around  $2\theta = 22.5$  in rice hull ash, silica (calcined at  $150\text{ }^{\circ}\text{C}$ ) and solid acid, corresponding to the diffraction of amorphous silica.<sup>24</sup> The sharp smaller peaks present in the rice hull ash were due to the presence of impurities in the sample.<sup>25</sup> The peaks ( $2\theta = 26.72, 32.50, 39.29$  and  $46.50$ , due to crystalline silica) in the XRD pattern of silica from the rice hull ash (Fig. 1c) indicates that crystalline silica can be produced from the rice hull ash by calcinations at relatively higher temperature.<sup>26</sup> Other reports confirmed that phase transformation is occurred at higher calcined temperature, which is consistence with the present case.<sup>27, 28</sup> Due to its high surface area, the amorphous silica (calcined at  $150\text{ }^{\circ}\text{C}$ ) was chosen as the raw material of the solid acid. As can be seen in the XRD characterization (Fig. 1d), the solid acid catalyst here is clearly in the form of amorphous silica.

##### 3.1.2 FT-IR analysis

The major chemical groups present in silica are identified by the FTIR spectra shown in Fig. 2. The band at  $465\text{ cm}^{-1}$  is attributed to the bending vibrations of Si-O-Si. The bands at  $831$  and  $1098\text{ cm}^{-1}$  are ascribed to the symmetric and

asymmetric stretching modes of Si-O-, respectively.<sup>29</sup> While the bands at 1066 and 1201  $\text{cm}^{-1}$  in the spectra of the solid acid can be assigned to the  $\text{SO}_2$  asymmetric and symmetric stretching modes, respectively.<sup>30</sup> The band at 667  $\text{cm}^{-1}$  can be attributed to the chelating structure of  $\text{SO}_4^{2-}$  groups.<sup>18</sup> It indicates that  $\text{SO}_4^{2-}$  groups are not in the free sulfuric acid state but linked on the surface of the activated solid acid. The broad band centered at 3450  $\text{cm}^{-1}$  was assigned to the -OH stretching mode.<sup>31</sup> Therefore, the FT-IR confirms that all the three samples consist of the silica particles. In addition, the  $-\text{SO}_3\text{H}$  groups were formed as the functional groups in the solid acid after sulfuric acid activation.

### 3.1.3 Solid state NMR analysis

The type and strength of acid sites are the fundamental properties of the solid acid. Trimethylphosphine (TMP) is a very useful probe molecule in authenticating the acid types such as Lewis or Brønsted acid sites in the solid acid surface.<sup>23</sup> Figure 3a illustrates the  $^{31}\text{P}$  single pulse spectrum obtained after adsorbing TMP onto the surface of solid acid. Two peaks at -2 and -60 ppm are observed in the spectrum. The former can be unambiguously assigned to TMP adsorbed on the Brønsted acid sites and the latter is generally originated from physisorbed TMP. It is obvious that the negligible amount of Lewis sites exists in the solid acid since no signal appears between -32 and -58 ppm.<sup>32</sup> Since no Lewis acid sites were detected by the TMP probe molecule and the resonance at 45 ppm is ascribed to the physisorbed trimethylphosphine oxide (TMPO),<sup>33</sup> the other two resonances at 55 and 72 ppm in

the  $^{31}\text{P}$  NMR spectrum of TMPO adsorbed on the solid acid can be both attributed to the Brønsted sites (Fig. 3b): the weakly acidic OH groups and the relatively strong acid sites  $-\text{SO}_3\text{H}$  groups, respectively.<sup>34</sup> The large chemical shift of 72 ppm indicates that the acid strength of the solid acid is stronger than that of HY with the Si/Al ratio of 3 (shown  $^{31}\text{P}$  chemical shifts of 65 ppm).<sup>35</sup> As a reliable NMR probe molecule, 2- $^{13}\text{C}$ -acetone can be used in conjunction with  $^{13}\text{C}$  MAS NMR chemical shift as a measure of relative acid strength of various solid acids.<sup>35</sup> The formation of a hydrogen bond between the acidic proton and the carbonyl oxygen of adsorbed acetone will cause a downfield shift of the carbonyl carbon. Besides the peaks associated with mesityl oxide (133, 53, 29 and 18 ppm),<sup>36</sup> two peaks at 219 and 230 ppm are observed in the  $^{13}\text{C}$  CP/MAS spectrum of acetone-2- $^{13}\text{C}$  adsorbed on the solid acid (Fig. 3c). The resonance at 113 ppm is due to the background of the probe. Similarly, the signal at 219 ppm is ascribed to acetone-2- $^{13}\text{C}$  adsorbed on the relatively weak acidic -OH groups and resonance at 230 ppm is due to acetone-2- $^{13}\text{C}$  adsorbed on the strong Brønsted acid sites ( $-\text{SO}_3\text{H}$  groups). The signal of 230 ppm indicates that the acid strength of the solid acid is weaker than that of 100%  $\text{H}_2\text{SO}_4$  (a  $^{13}\text{C}$  chemical shift of 245 ppm).<sup>37</sup>

### 3.1.4 TEM

The nano-size and spherical structure of silica from the rice hull ash and the solid acid was confirmed by transmission electron microscopy (TEM) images (Fig. 4). As Fig. 4 shown, the sphere size of two samples was about 50-100 nm, which indicates

that the solid acid is a nano-sized catalyst.

### 3.2. Catalytic reaction

In order to evaluate the activity of the solid acid in the reaction, a comparative study was carried out between the solid acid prepared from rice hull ash, concentrated  $\text{H}_2\text{SO}_4$  and typical solid acid  $\text{SO}_4^{2-}/\text{ZrO}_2$  (Table 3). The reaction used was the transesterification of soybean oil (10 mmol) with methanol (120 mmol) under reflux. The same amount (0.015 g) of all the catalysts was used in the reactions. As can be seen in table 3, the solid acid from rice hull ash shows lower activity than that of concentrated  $\text{H}_2\text{SO}_4$ , but still higher than that of  $\text{SO}_4^{2-}/\text{ZrO}_2$  catalyst. It clearly suggests that the solid acid should be considered as one of the best choice for the economically convenient, user-friendly catalyst for acid catalysis reaction.

The catalytic reusability of the solid acid from rice hull ash was evaluated by running the transesterification reaction ten times. The same catalyst was directly used in each time without any pretreatment. As shown in Fig. 5, the yield of biodiesel gradually decreased from 92% to 51% in the ten cycles. From Table 2 we can see that the loss in surface area, pore volume and acid sites of the spent catalyst suggests that deactivation arises as a result of pore blocking by some reaction intermediate or product species. When the ten cycles were over, the spent catalyst was obtained. And then the regeneration process was performed to reactivate the spent catalyst. After

washing with acetone and then drying at 120 °C under the vacuum for 5 h, the total acid density increased from 2.32 to 3.96 mmol/g, it mostly recovered its original activity (4.05 mmol/g of fresh catalyst), which confirms its reusability as catalyst for biodiesel production (Table 2).<sup>38</sup> Therefore, the simple regeneration method is helpful to the catalyst application in a fixed bed of the continuous product system.

#### 4. Conclusions

In summary, a nano-sized solid acid was synthesized from rice hull ash by acid activation. Our characterization results show that the solid acid is the amorphous silica with -OH and -SO<sub>3</sub>H functional acid groups. The TEM images display the particle size range of the solid acid catalyst is 50-100 nm. The catalytic results indicated that the solid acid catalyst is very active at the suitable conditions for the transesterification of soybean oil with methanol. The reusability of the solid acid was also confirmed in the transesterification reaction. It is possible that this promising solid acid can be widely used in the acid catalysis reaction.

#### Acknowledgments

We acknowledge the financial supports from the Science and Technology Plan of Wuhan (201060723317), the Open Research Fund of Hubei Key Laboratory for Efficient Utilization and Agglomeration of Metallurgic Mineral Resources and the Open Research Fund of Key Laboratory for Ferrous Metallurgy and Resources Utilization of Ministry of Education (FMRU201209).

## References

- 1 P. T. Anastas and M. M. Kirchhoff, *Acc. Chem. Res.*, 2002, **35**, 686–694.
- 2 J. M. Desimone, *Science*, 2002, **297**, 799–803.
- 3 P. T. Anastas and J. B. Zimmermann, *Environ. Sci. Technol.*, 2003, **37**, 94–101.
- 4 E. Lotero, Y. Liu, D. E. Lopez, A. Suwannakaran, D. A. Bruce and J. G. Goodwin, *Ind. Eng. Chem. Res.*, 2005, **44**, 5353–5363.
- 5 A.P. S. Chouhan and A. K. Sarma, *Renew. Sust. Energ. Rev.*, 2011, **15**, 4378–4399.
- 6 A. Corma and H. Garcia, *Catal. Today*, 1997, **38**, 257–308.
- 7 T. Okuhara, *Chem. Rev.*, 2002, **102**, 3641–3666.
- 8 J.A. Melero, J. Iglesias and G. Morales, *Green Chem.*, 2009, **11**, 1285–1308.
- 9 A. Corma and A. Martinez, *Adv. Mater.*, 1995, **7**, 137–144.
- 10 M.A. Harmer and Q. Sun, *Appl. Catal. A Gen.*, 2001, **221**, 45–62.
- 11 M.A. Harmer, Q. Sun, A.J. Vega, W.E. Farneth, A. Heidekum and W.F. Hoelderich, *Green Chem.*, 2000, **2**, 7–14.
- 12 A.A. Kiss, A.C. Dimian and G. Rothenberg, *Adv. Synth. Catal.*, 2006, **348**, 75–81.
- 13 V.L. Budarin, J.H. Clark, R. Luque and D.J. Macquarrie, *Chem. Commun.*, 2007, **6**, 634–636.
- 14 S. Suganuma, K. Nakajima, M. Kitano, D. Yamaguchi, H. Kato, S. Hayashi and M. Hara, *J. Am. Chem. Soc.*, 2008, **130**, 12787–12793.
- 15 D. Zeng, S. Liu, W. Gong, G. Wang, J. Qiu and Y. Tian, *Catal. Commun.*, 2013, **40**, 5–8.
- 16 J.M. Riego, Z. Sedin, J.M. Zaldivar, N.C. Marzianot and C. Tortatot, *Tetrahedron*

- Lett.*, 1996, **37**, 513-516.
- 17 S.-N. Masoud and J. Jaber, *Comb. Chem. High T. Scr.*, 2012, **15**, 705-712.
- 18 H.R. Shaterian, M. Ghashang and M. Feyzi, *Appl. Catal., A Gen.*, 2008, **345**, 128-133.
- 19 S.R. Kamath and A. Proctor, *Cereal Chem.* 1998, **75**, 484-487.
- 20 V.P. Della, I. Kühn and D. Hotza, *Mater. Lett.*, 2002, **57**, 818-821.
- 21 T. Witoon, M. Chareonpanich and J. Limtrakul, *Mater. Lett.*, 2008, **62**, 1476-1479.
- 22 S. Huang, S. Jing, J.F. Wang, Z.W. Wang and Y. Jin, *Powder Technol.*, 2001, **117**, 232-238.
- 23 J.F. Haw, J.H. Zhang, K. Shimizu, T.N. Venkatraman, D. Luigi, W. Song, D.H. Barich and J.B. Nicholas, *J. Am. Chem. Soc.*, 2000, **122**, 12561-12570.
- 24 X.Ma, B. Zhou, W. Gao, Y. Qu, L. Wang, Z. Wang and Y. Zhu, *Powder Technol.*, 2012, **217**, 497-501.
- 25 U. Kalapathy, A. Proctor and J. Shultz, *Biores. Technol.*, 2002, **85**, 285-289.
- 26 M. Kima, S.H. Yoon, E. Choic and B. Gil, *LWT*, 2008, **41**, 701-706.
- 27 M. Sarangi, P. Nayak and T.N. Tiwari, *Compos. Part B-Eng.*, 2011, **42**, 1994-1998.
- 28 H. Hamdan., M. N. M. Muhid, S. Endud, E. Listiorini and Z. Ramli, *J. Non-Cryst. Solids*, 1997, **211**, 126-131.
- 29 V.S. Braga, J.A. Dias, S.C.L. Dias and J.L. Macedo, *Chem. Mater.*, 2005, **17**, 690-695.
- 30 W. Zhao, B. Yang, C. Yi, Z. Lei and J. Xu, *Ind. Eng. Chem. Res.*, 2010, **49**, 12399-12404.



- 31 W.P. Rothwell, W. Shen and J.H. Lunsford, *J. Am. Chem. Soc.*, 1984, **106**, 2452-2453.
- 32 J.H. Lunsford, W.P. Rothwell and W. Shen, *J. Am. Chem. Soc.*, 1985, **107**, 1540-1547.
- 33 E.F. Rackiewicz, A.W. Peters, R.F. Wormsbecher, K.J. Sutovich and K.T. Mueller, *J. Phys. Chem. B*, 1998, **102**, 2890-2896.
- 34 Q. Zhao, W.H. Chen, S.J. Huang, Y.C. Wu, H.K. Lee and S.B. Liu, *J. Phys. Chem. B*, 2002, **106**, 4462-4469.
- 35 J.F. Haw, J.B. Nicholas, T. Xu, L.W. Beck and D.B. Ferguson, *Acc. Chem. Res.*, 1996, **29**, 259-267.
- 36 T. Xu, E.J. Munson and J.F. Haw, *J. Am. Chem. Soc.*, 1994, **116**, 1962-1972.
- 37 A. I. Biaglow, R.J. Gorte and D. White, *J. Catal.*, 1994, **150**, 221-224.
- 38 B. A. D. Neto, M. B. Alves, A. A.M. Lapis, F. M. Nachtigall, M. N. Eberlin, J. Dupont and P.A.Z. Suarez, *J. Catal.*, 2007, **249**, 154-161.

### Figure Captions

Fig. 1. XRD patterns of (a) rice hull ash, (b) silica (calcined at 150 °C), (c) silica (calcined at 1000 °C) and (d) the solid acid. ▼ denotes peaks of crystalline silica, ▽ denotes peak of amorphous silica.

---

Fig. 2. FT-IR spectra of (a) rice hull ash, (b) silica (calcined at 150 °C) and (c) the solid acid.

Fig. 3.  $^{31}\text{P}$  single pulse with  $^1\text{H}$  decoupling MAS spectra of (a) TMP and (b) TMPO adsorbed on the solid acid; (c)  $^{13}\text{C}$  CP/MAS NMR spectra of 2- $^{13}\text{C}$ -acetone (0.2 mmol/g) adsorbed on the solid acid. The asterisk denotes spinning sidebands.

Fig. 4. TEM of (a) silica (calcined at 150 °C) and (b) the solid acid.

Fig. 5. The recycling of the solid acid from rice hull ash for the transesterification reaction. Reaction condition: 10 mmol soybean oil; 120 mmol methanol; 0.015 g catalyst; 80 °C.

Table 1 Chemical composition of rice hull ash (wt%)

Sample	SiO <sub>2</sub>	CaO	Na <sub>2</sub> O	Al <sub>2</sub> O <sub>3</sub>	MgO
rice hull ash	90.15	0.84	0.70	0.26	0.05

Table 2 Pore structure and total acid density of rice hull ash and solid acid from rice hull ash (fresh, spent and regenerated).

Sample	$S_{\text{BET}}$ ( $\text{m}^2/\text{g}$ )	$V_{\text{tot}}$ ( $\text{cm}^3/\text{g}$ )	$D$ (nm)	Total acid density (mmol /g)
Rice hull ash	49	0.023	0.58	0.01
Solid acid(fresh)	203	0.756	2.16	4.05
Solid acid (spent)	143	0.549	2.01	2.32
Solid acid (regenerated)	199	0.735	2.11	3.96

$S_{\text{BET}}$ , specific surface area from BET method;  $V_{\text{tot}}$ , total pore volume;  $D$ , average pore diameter.

Table 3 Textural properties and the catalytic performance of the various catalysts.

Catalysts	$S_{\text{BET}}$ ( $\text{m}^2/\text{g}$ )	$V_{\text{tot}}$ ( $\text{cm}^3/\text{g}$ )	$D$ (nm)	Total density ( $\text{mmol}/\text{g}$ )	acid Yield (%)	TOF ( $\text{h}^{-1}$ )
Solid acid	203	0.246	1.16	4.05	92	75.7
$\text{SO}_4^{2-}/\text{ZrO}_2$	155	0.224	4.88	4.42	87	65.6
$\text{H}_2\text{SO}_4(98\%)$	-	-	-	20.40	96	125.5

$S_{\text{BET}}$ , specific surface area from BET method;  $V_{\text{tot}}$ , total pore volume;  $D$ , average pore diameter.

TOF(Turn over frequency)was calculated on the data of the mol of converted reactant, the mol of acid sites and reaction equilibrium time.

Reaction condition: 10 mmol soybean oil; 120 mmol methanol; 0.015 g catalyst; 80 °C.

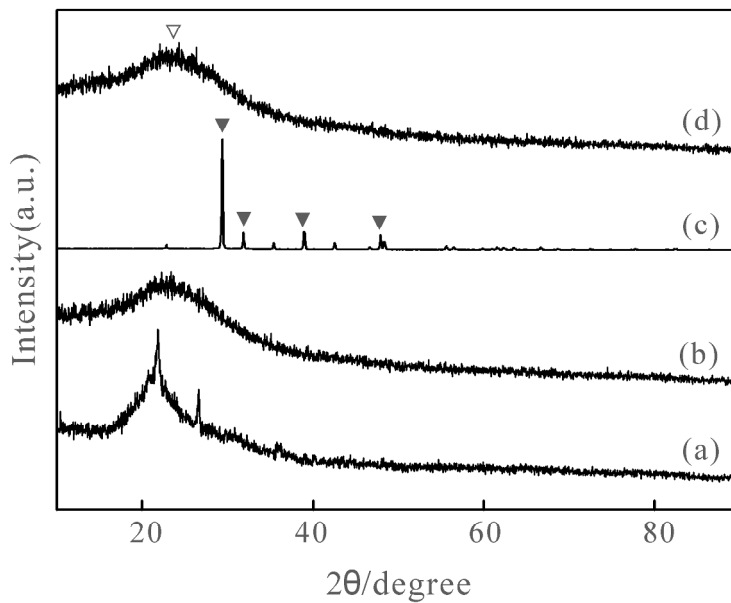


Fig. 1. XRD patterns of (a) rice hull ash, (b) silica (calcined at 150 °C), (c) silica (calcined at 1000 °C) and (d) the solid acid.  $\blacktriangledown$  denotes peaks of crystalline silica,  $\nabla$  denotes peak of amorphous silica.  
292x202mm (300 x 300 DPI)

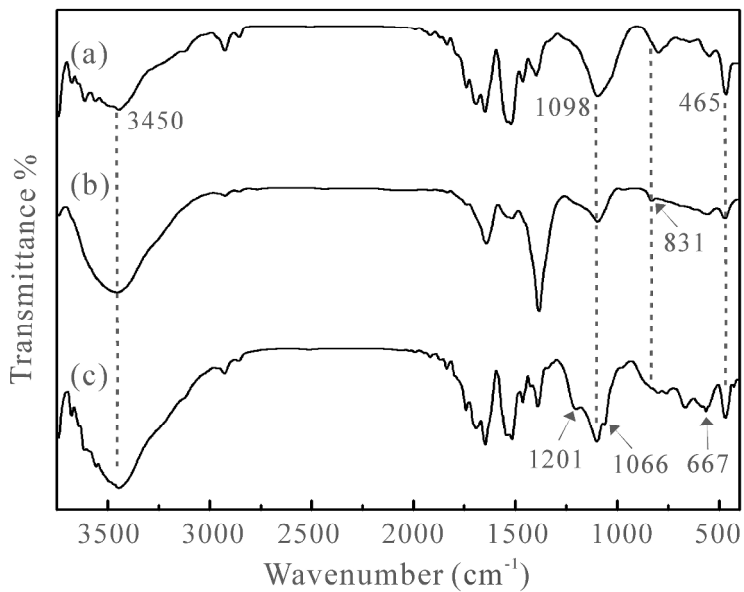


Fig. 2. FT-IR spectra of (a) rice hull ash, (b) silica (calcined at 150 °C) and (c) the solid acid.  
292x202mm (300 x 300 DPI)

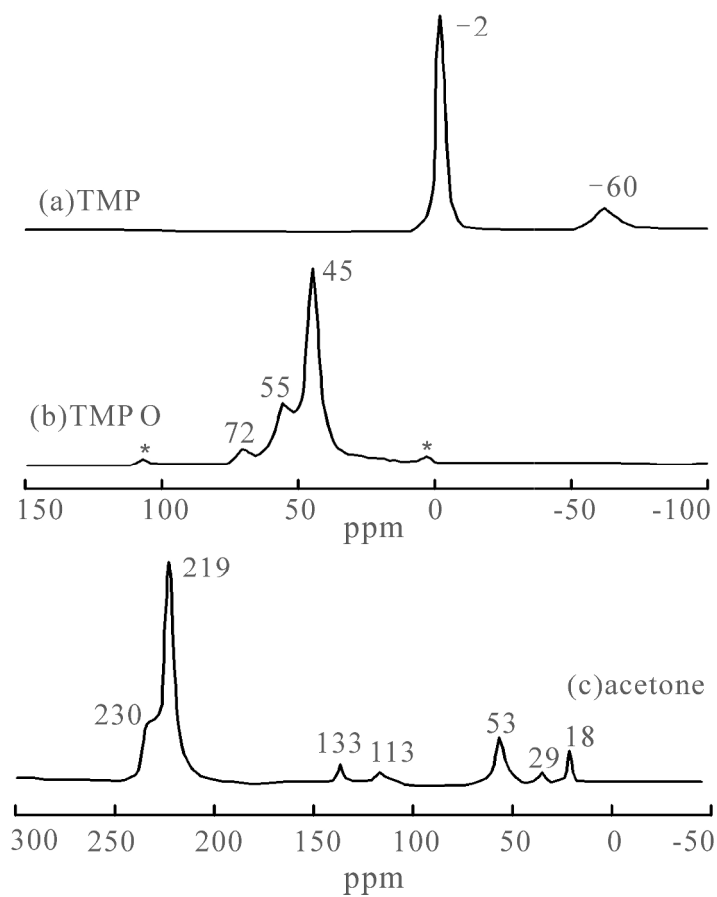


Fig. 3.  $^{31}\text{P}$  single pulse with  $^1\text{H}$  decoupling MAS spectra of (a) TMP and (b) TMPO adsorbed on the solid acid; (c)  $^{13}\text{C}$  CP/MAS NMR spectra of 2- $^{13}\text{C}$ -acetone (0.2 mmol/g) adsorbed on the solid acid. The asterisk denotes spinning sidebands.  
283x273mm (300 x 300 DPI)



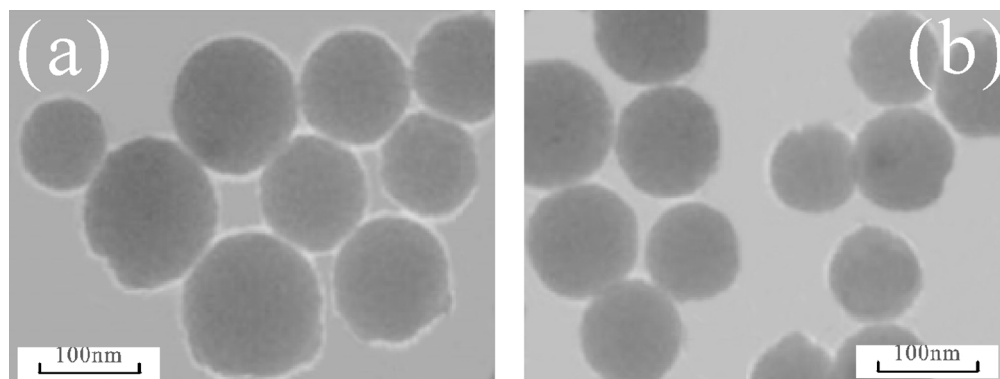


Fig. 4. TEM of (a) silica (calcined at 150 °C) and (b) the solid acid.  
125x47mm (300 x 300 DPI)

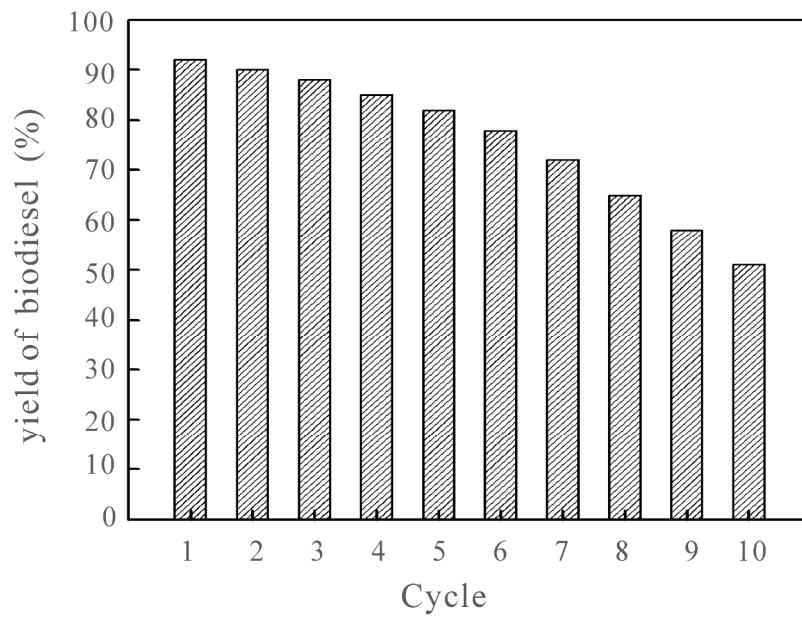
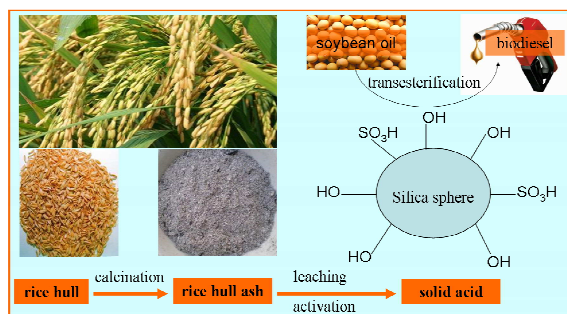


Fig. 5. The recycling of the solid acid from rice hull ash for the transesterification reaction. Reaction condition: 10 mmol soybean oil; 120 mmol methanol; 0.015 g catalyst; 80 °C.  
292x202mm (300 x 300 DPI)



A nano-sized solid acid was synthesized from rice hull ash by acid activation. The solid acid is the amorphous silica with -OH and -SO<sub>3</sub>H functional acid groups and this catalyst exhibits excellent activity and recyclability for biodiesel production.